Tunable microwave signal generator with an optically-injected 1310nm QD-DFB laser

Antonio Hurtado,[1,2*] Jesse Mee,[1] Mohsen Nami,[1] Ian D. Henning,[2] Michael J. Adams,[2] and Luke F. Lester[1]

[1]*Center for High Technology Materials, University of New Mexico, 1313 Goddard SE, Albuquerque, New Mexico, 87106, USA*

[2]*School of Computer Science and Electronic Engineering, University of Essex, Wivenhoe Park, Colchester, Essex, CO4 3SQ, UK*

[*]*ahurta01@unm.edu*

Abstract: Tunable microwave signal generation with frequencies ranging from below 1 GHz to values over 40 GHz is demonstrated experimentally with a 1310nm Quantum Dot (QD) Distributed-Feedback (DFB) laser. Microwave signal generation is achieved using the period 1 dynamics induced in the QD DFB under optical injection. Continuous tuning in the positive detuning frequency range of the quantum dot's unique stability map is demonstrated. The simplicity of the experimental configuration offers promise for novel uses of these nanostructure lasers in Radio-over-Fiber (RoF) applications and future mobile networks.

OCIS codes: (250.5960) Semiconductor lasers; (140.3490) Lasers, distributed-feedback; (350.4010) Microwaves; (250.5590) Quantum-well, -wire and -dot devices.

References and links

1. X. Q. Qi and J. M. Liu, "Photonic microwave applications of the dynamics of semiconductor lasers," IEEE J. Sel. Top. Quantum Electron. **17**(5), 1198–1211 (2011).
2. S. C. Chan, "Analysis of an optically injected semiconductor laser for microwave generation," IEEE J. Quantum Electron. **46**(3), 421–428 (2010).
3. S. C. Chan, S. K. Hwang, and J. M. Liu, "Radio-over-fiber AM-to-FM upconversion using an optically injected semiconductor laser," Opt. Lett. **31**(15), 2254–2256 (2006).
4. Y. S. Juan and F. Y. Lin, "Photonic generation of broadly tunable microwave signals utilizing a dual-beam optically injected semiconductor laser," IEEE Photon. J. **3**(4), 644–650 (2011).
5. M. Pochet, T. Locke, and N. G. Usechak, "Generation and modulation of a millimeter-wave subcarrier on an optical frequency generated via optical injection," IEEE Photon. J. **4**(5), 1881–1891 (2012).
6. T. B. Simpson, J.-M. Liu, M. AlMulla, N. Usechak, and V. Kovanis, "Tunable photonic microwave oscillator self-locked by polarization-rotated optical feedback" IEEE International Frequency Control Symposium, Proceedings, 1–5, (2012).
7. A. Quirce and A. Valle, "High-frequency microwave signal generation using multi-transverse mode VCSELs subject to two-frequency optical injection," Opt. Express **20**(12), 13390–13401 (2012).
8. J. F. Hayau, O. Vaudel, P. Besnard, F. Lelarge, B. Rousseau, L. Le Gouezigou, F. Pommereau, F. Poingt, O. Le Gouezigou, A. Shen, G.-H. Duan, O. Dehaese, F. Grillot, R. Piron, S. Loualiche, A. Martinez, K. Merghem, and A. Ramdane, "Optical injection of quantum dot and quantum dash semiconductor lasers" European Conf. of Laser and Electrooptics, CLEO-Europe 2009, Munich, 14–19 June 2009.
9. E. Sooudi, G. Huyet, J. G. McInerney, F. Lelarge, K. Merghem, R. Rosales, A. Martinez, A. Ramdane, and S. P. Hegarty, "Injection-locking properties of InAs/InP-based mode-locked quantum-dash lasers at 21 GHz," IEEE Photon. Technol. Lett. **23**(20), 1544–1546 (2011).
10. T. Erneux, E. A. Viktorov, B. Kelleher, D. Goulding, S. P. Hegarty, and G. Huyet, "Optically injected quantum-dot lasers," Opt. Lett. **35**(7), 937–939 (2010).
11. B. Kelleher, D. Goulding, S. P. Hegarty, G. Huyet, E. A. Viktorov, and T. Erneux, *Optically Injected Single-Mode Quantum Dot Lasers in Quantum Dot Devices* (Springer, 2012), Chap. 1, pp. 1–22
12. A. Hurtado, M. Nami, I. D. Henning, M. J. Adams, and L. F. Lester, "Bistability patterns and nonlinear switching with very high contrast ratio in a 1550nm quantum dash semiconductor laser," Appl. Phys. Lett. **101**(16), 161117 (2012).
13. F. van Dijk, B. Charbonnier, S. Constant, A. Enard, S. Fedderwitz, S. Formont, I. F. Lealman, F. Lecoche, F. Lelarge, D. Moodie, L. Ponnampalam, C. Renaud, M. J. Robertson, A. J. Seeds, A. Stohr, and M. Weiss, "Quantum dash mode-locked lasers for millimeter wave signal generation and transmission" 23rd Annual Meeting of the IEEE Photonics Society, 187–188 (2010).

#185425 - $15.00 USD Received 15 Feb 2013; revised 3 Apr 2013; accepted 15 Apr 2013; published 25 Apr 2013

14. N. Yamamoto, K. Akahane, T. Kawanishi, H. Sotobayashi, Y. Yoshioka, and H. Takai, "Characterization of wavelength-tunable quantum dot external cavity laser for 1.3-μm-waveband coherent light sources," Jpn. J. Appl. Phys. **51**(2), 02BG08 (2012).
15. G. Carpintero, M. G. Thompson, R. V. Penty, and I. H. White, "Low noise performance of passively mode-locked 10-GHz quantum-dot laser diode," IEEE Photon. Technol. Lett. **21**(6), 389–391 (2009).
16. M. J. Fice, E. Rouvalis, F. van Dijk, A. Accard, F. Lelarge, C. C. Renaud, G. Carpintero, and A. J. Seeds, "146-GHz millimeter-wave radio-over-fiber photonic wireless transmission system," Opt. Express **20**(2), 1769–1774 (2012).
17. M. Pochet, N. A. Naderi, Yan Li, V. Kovanis, and L. F. Lester, "Tunable photonic oscillators using optically injected quantum-dash diode lasers," IEEE Photon. Technol. Lett. **22**(11), 763–765 (2010).
18. P. Bhattacharya, D. Klotzkin, O. Qasaimeh, W. Zhou, S. Krishna, and D. Zhu, "High-speed modulation and switching characteristics of In(Ga)As-Al(Ga)As self-organized quantum-dot lasers," IEEE J. Sel. Top. Quantum Electron. **6**(3), 426–438 (2000).
19. H. Y. Liu, T. J. Badcock, K. M. Groom, M. Hopkinson, M. Gutiérrez, D. T. Childs, C. Jin, R. A. Hogg, I. R. Sellers, D. J. Mowbray, M. S. Skolnick, R. Beanland, and D. J. Robbins, "High-performance 1.3μm InAs/GaAs quantum-dot lasers with low threshold current and negative characteristic temperature," Proc. SPIE Vol. **6184**, 618417 (2006).
20. T. C. Newell, D. J. Bossert, A. Stintz, B. Fuchs, K. J. Malloy, and L. F. Lester, "Gain and linewidth enhancement factor in InAs quantum-dot laser diodes," IEEE Photon. Technol. Lett. **11**(12), 1527–1529 (1999).
21. S. Wieczorek, B. Krauskopf, T. B. Simpson, and D. Lenstra, "The dynamical complexity of optically injected semiconductor lasers," Phys. Rep. **416**(1-2), 1–128 (2005).
22. H. Su, L. Zhang, A. L. Gray, R. Wang, T. C. Newell, K. J. Malloy, and L. F. Lester, "High External Feedback Resistance of Laterally Loss-Coupled Distributed Feedback Quantum Dot Semiconductor Lasers," IEEE Photon. Technol. Lett. **15**(11), 1504–1506 (2003).
23. L. Zhang, R. Wang, Z. Zou, A. Gray, L. Olana, T. Newell, D. Webb, P. Varangis, and L. F. Lester, "InAs quantum dot DFB lasers on GaAs for uncooled 1310 nm fiber communications" Optical Fiber Communication Conference (OFC), Atlanta, GA (2003).
24. H. Su and L. F. Lester, "Dynamic properties of quantum dot distributed feedback lasers: high speed, linewidth and chirp," J. Phys. D Appl. Phys. **38**(13), 2112–2118 (2005).
25. A. Hurtado, A. Quirce, A. Valle, L. Pesquera, and M. J. Adams, "Nonlinear dynamics induced by parallel and orthogonal optical injection in 1550 nm Vertical-Cavity Surface-Emitting Lasers (VCSELs)," Opt. Express **18**(9), 9423–9428 (2010).

1. Introduction

The study of photonic approaches for the generation of microwave and millimeter-wave (mm-wave) signals has recently received considerable attention. These techniques offer important advantages in comparison to traditional ones based on electronic circuitry, including low cost, tunability, reduced complexity, and lower energy consumption. Besides, photonic techniques are indeed promising to overcome the limited frequency response of electronic components and permit the transmission of microwave signals over long distances with optical fibers. Thus, the combination of microwave and photonic technologies for the development of stable and tunable photonic microwave sources is expected to play a key role in a wide range of future applications. These include Radio-over-fiber (ROF) technologies for optical wireless networks, 4G mobile communications systems, satellite telecommunication systems, etc. (for a review on the topic see [1] and references therein).

Various optical techniques using semiconductor lasers for the generation of microwave signals have been demonstrated, namely optical heterodyne detection, dual-mode lasing, mode-locking and optical injection (see [1] and references therein). In particular, the latter approach considers the use of the period 1 (P1) dynamics induced in a semiconductor laser, usually referred to as the Slave Laser (SL) when subject to external optical injection from another laser, known as the Master Laser (ML). Under certain conditions, the ML's light perturbs the SL's output making it exhibit periodic oscillations in the microwave frequency range. By controlling the injection strength and the initial frequency detuning between the ML and SL, these generated microwave signals can be tuned over a wide range of frequencies, from a few GHz to values well into the mm-wave band [1–6]. Several works have demonstrated high frequency, tunable and narrow linewidth microwave signals using semiconductor lasers under single and double beam injection configurations [1–6] and different laser structures, including edge-emitting [2–6] and vertical-cavity devices [7] with Quantum Well (QW) active regions have been studied.

#185425 - $15.00 USD Received 15 Feb 2013; revised 3 Apr 2013; accepted 15 Apr 2013; published 25 Apr 2013

Additionally, in recent years the analysis of optically-injected nanostructure lasers, such as quantum dash (QDash) and quantum dot (QD) devices has undergone considerable research effort. Several works have studied the injection locking, nonlinear dynamics and bistability occurring in such devices [8–12]. Yet, the use of nanostructure lasers for microwave signal generation has focused on mode-locking [13–15] or optical heterodyning [16] techniques whilst optical injection has not attracted much attention. Apart from a recent work using a 1550 nm Fabry-Perot QDash laser [17], we are not aware of other studies either with QDash or QD devices, especially single-mode emitters. Due to their theoretically superior properties, such as ultrafast carrier dynamics, reduced temperature dependence, etc. (see for instance [18–20]), nanostructure lasers are expected to play a key role as high-performance sources in a variety of future applications. Specifically, the present work investigates the generation of tunable microwave signals using the period 1 dynamics induced in an optically-injected 1310 nm QD DFB laser. We demonstrate microwave signal generation over a 5-octave range, with complete tunability from frequencies below 1GHz to over 40 GHz. As we will show, the stability map of the QD DFB laser of this work exhibits only P1 dynamics outside the locking range. Regions of more complex dynamics (such as period 2 or chaos) appearing in QW devices [21] are not observed. Such response guarantees the total use of the whole positive frequency detuning range of the coupled laser system for microwave signal generation.

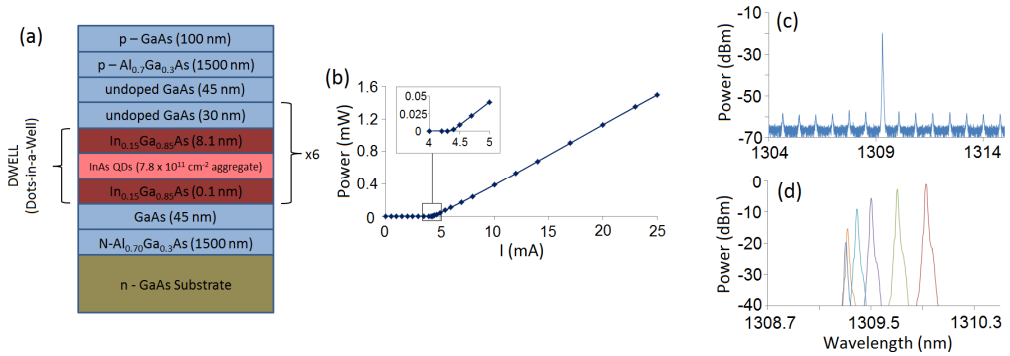

Fig. 1. (a) Epitaxial layer structure of the QD DFB laser. (b) LI curve at 298 K. Optical spectra of the device when biased with 4.6 mA (a) and with currents from 5 to 20 mA (d).

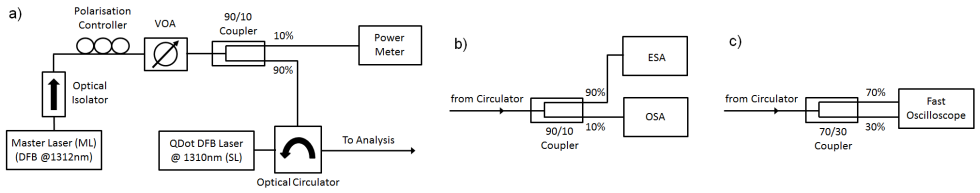

Fig. 2. Experimental setup: (a) main body; (b,c) analysis stages for the study of the electrical and optical spectra (b) and the time response (c).

2. Experimental setup

The device used in this work is a laterally-loss coupled DFB QD laser with emission at 1310 nm. The device has a cavity of 300 µm with asymmetrically HR-HR coated facets with 80% and 95% front and back facet reflectivities. A chromium grating with grating pitch of 200 nm facilitates distributed reflectivity. Such structure provides single mode emission with high Side Mode Suppression Ratio (SMSR) and suppresses excited state FP lasing. The epitaxial layer structure of the 1310 nm-QD DFB laser is depicted in Fig. 1(a). The active region consists of six 9.1 nm-thick InAs/InGaAs dots-in-a-well (DWELL) layers separated by 30 nm GaAs barriers. Complete details regarding the QD DFB laser's structure, as well as information on importance device parameters such as the relaxation oscillation frequency,

#185425 - $15.00 USD Received 15 Feb 2013; revised 3 Apr 2013; accepted 15 Apr 2013; published 25 Apr 2013

damping rate, linewidth and linewidth enhancement factor, etc. can be found in [22–24]. The LI curve of the device at 298 K is included in Fig. 1(b) giving a threshold current of approx. I_{th} = 4.4 mA. Measured optical spectra of the device when biased just (with 4.6 mA) and well-above threshold (from 5 to 20 mA) are shown respectively in Figs. 1(c) and 1(d), exhibiting single-mode emission at around 1310 nm. Figure 1(c) also shows the attenuated longitudinal cavity modes of the device which are separated approximately 0.8nm; a measured SMSR in excess of 35 dB was observed with the devices biased just above threshold.

Figure 2(a) plots the main part of the experimental setup developed to inject light from a commercially available 1310nm QW laser (ML) into the 1310nm QD DFB laser (SL). An Optical Isolator is included after the ML to avoid undesired reflections leading to spurious results. A polarization controller and a variable optical attenuator (VOA) are used to control the polarization and optical power of the ML's light, respectively A 90/10 fiber directional coupler divides the optical path into two branches. The 10% port is connected to a power meter to monitor the injected power. The 90% port is injected into the SL via a polarization maintaining optical circulator. The SL's reflective output is collected and directed to the analyses part of the setup, plotted in Figs. 2(b) and 2(c). Specifically, Fig. 2(b) plots the setup designed to analyze the SL's optical and electrical spectra. In this first case a 10/90 coupler is connected to the circulator to divide the SL's output into two paths for its simultaneous optical and electrical analysis using an Optical and an Electrical Spectrum Analyzer (OSA and ESA). Figure 2(c) plots the setup designed for the analysis of the time dependent response. Now, a 30/70 coupler is included after the circulator and its two outputs are both simultaneously connected to a fast oscilloscope. The 30% branch is connected to the input optical signal port of the scope whereas the 70% line is connected to the triggering port of the scope.

3. Results and discussion

A tool traditionally used in the analysis of optically-injected lasers is the so-called stability map. This map plots the different behaviors induced in the SL by the ML's injection in the plane of injection power (P_{inj}) versus frequency detuning (Δf). One of these is referred to as injection locking, where the SL's wavelength follows that of the ML. However, injection locking only occurs in a small area in the map. Outside that range, a rich variety of nonlinear dynamics may occur, including periodic dynamics such as period 1 (P1), period 2 (P2), as well as regions of chaotic dynamics, excitability, etc. (for a review see [21]). Typically reported stability maps for optically-injected QW lasers (either for planar [21] or vertical-cavity devices [25]) exhibit in the positive detuning range a wide region of P1 dynamics surrounding large islands of P2 and chaos. In contrast, stability maps reported very recently for an optically-injected QD DFB laser [10,11] have shown a completely different shape for the injection locking range and observed nonlinear dynamics.

Figure 3(a) plots the measured stability map for the 1310-nm QD DFB laser used in this work when biased with 55 mA (≈12.5 x I_{th}). Several interesting features appear in Fig. 3(a). First, the injection locking region shows a peculiar asymmetric shape around the Δf = 0 GHz plane. This differs to that observed in QW devices [21] where the Hopf bifurcation in the upper limit typically crosses the zero detuning point and exhibits a rich variety of complex nonlinear dynamics. In fact, the map in Fig. 3(a) shows more similarities to that reported in [10,11] for another QD DFB device. As in [10,11] the stable locking range also extends well into the positive frequency range and does not exhibit a minimum point crossing the zero detuning line. Still, important contrasts are found with the results reported in [10,11]. The large region of P2 dynamics reported in [11] do not appear and only P1 dynamics are measured outside the stable locking range. Moreover, opposite to the typical results reported for QW laser sources [21] [25], the QD DFB analyzed here does not display additional islands of P2 and chaos outside the locking range. Therefore, a large undisrupted region of P1 dynamics is present for the entire positive detuning range (for values exceeding + 3.5 GHz). In this region, the QD DFB laser's output exhibits periodic oscillations at frequencies

#185425 - $15.00 USD Received 15 Feb 2013; revised 3 Apr 2013; accepted 15 Apr 2013; published 25 Apr 2013

covering the microwave range leading to the potential use of this device for microwave signal generation purposes.

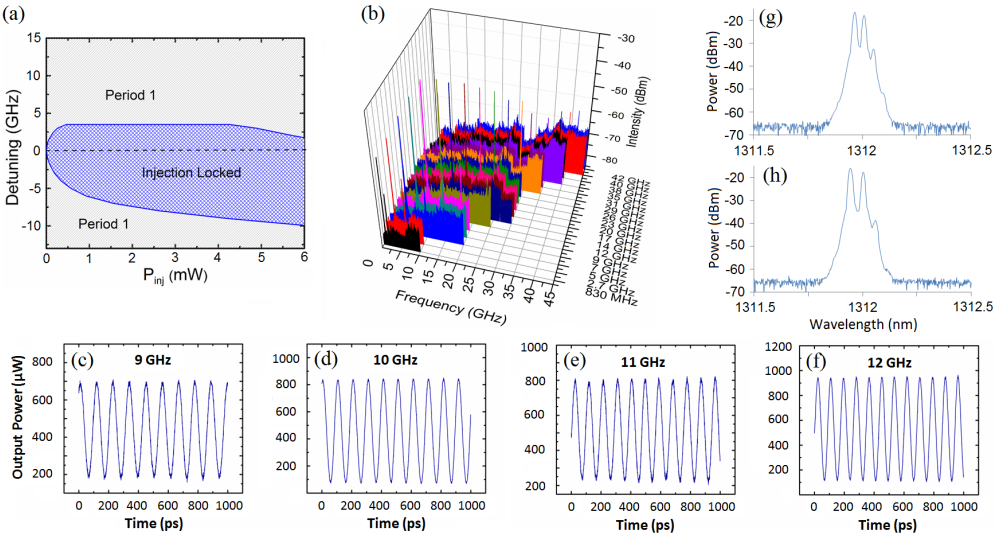

Fig. 3. (a) Stability map of the QD DFB laser at I_{Bias} = 55mA. (b) Superimposed electrical spectra generating signals with frequencies from 830 MHz to 42 GHz. (c-f) Time traces showing tunability of the signals from 9 to 12 GHz ({P_{inj}, Δf} are equal to: (c) {5.28 mW, 5 GHz}, (e) {5.6 mW, 6 GHz}, (d) {6.36 mW, 7 GHz} and (e) {6.4 mW, 8.5 GHz}). (g-h) SSB microwave signals with frequencies equal to 7.5 GHz (g) and 10 GHz (h).

The frequency of the generated signals depends strongly on the configured initial conditions, namely the initial frequency detuning between the ML and SL (Δf) and the injection strength (P_{inj}) [1–7]. Thus, a generated microwave signal could be tuned along this vast region of P1 dynamics by just controlling these two parameters. This is illustrated in Figs. 3(b)-3(f) plotting the various superimposed electrical spectra [Fig. 3(b)] and time series [Figs. 3(c)-3(f)] measured at the SL's output for several values of $\{P_{inj}, \Delta f\}$. Figure 3(b) shows the generation of microwave signals with frequencies ranging from below 1 GHz to values exceeding 40 GHz. The time traces shown in Figs. 3(c)-3(f) illustrate the tunability of a generated microwave signal from 9 to 12 GHz just by changing P_{inj} and Δf. In all four cases, depicted in Figs. 3(c)-3(f), pure, high amplitude and high quality sinusoidal periodical signals were measured at the QD DFB laser's output. Therefore, from Fig. 3 we can conclude that with the simple experimental configuration of this work microwave signals from a few GHz (and even lower) to more than 40 GHz can be generated yielding an inexpensive and highly tunable microwave source. In addition, the lack of regions of unwanted dynamics (P2 or chaos) in the stability map offers promise for a much simpler tuning control of the generated microwave signals in comparison to systems based on QW semiconductor lasers; essentially, the potential for tuning gaps in this QD DFB is eliminated.

Additionally, Single-Side Band (SSB) modulation is also achieved with the proposed configuration as shown in Figs. 3(g) and 3(h). These plots show the measured optical spectra for the situations where 7.5 GHz [Fig. 3(g)] and 10 GHz [Fig. 3(h)] microwave signals are generated. The two spectra in Figs. 3(g)-3(h) show the appearance of a SSB on the longer wavelength side of the resonant wavelengths of the ML and SL. The frequency separation at which this SSB appears corresponds in fact with the frequency of the microwave generated signal: 7.5 and 10 GHz, respectively. Such SSB response is explained from the increase of the SL's resonant wavelength with injection strength which favors the side-band in the longer wavelength side relative to the one in the shorter-wavelength side. This effect finally leads to the achievement of SSB modulation which is of interest for RoF transmission systems as it

#185425 - $15.00 USD Received 15 Feb 2013; revised 3 Apr 2013; accepted 15 Apr 2013; published 25 Apr 2013

reduces the power penalty caused by chromatic dispersion in optical fibers in comparison with Double Side Band (DSB) modulation [1].

The frequency and amplitude characteristics of the microwave signals generated with the optically-injected 1310nm-QD DFB laser of this work have also been analyzed. The device was biased with a current of 55 mA (≈12.5 x I_{th}). Figure 4(a) shows an experimental 3D map data plotting the evolution of the oscillation frequency of the generated microwave signal as a function of P_{inj} and Δf. The vast region of period 1 dynamics appearing in the positive frequency detuning range is the focus of this plot; thus, only results for that range are represented in Fig. 4(a) from which several conclusions can be extracted. The first one is that microwave signals with frequencies going from under 1 GHz to values up to approx. 40 GHz were continuously generated with the optically-injected QD DFB laser. Also, for a particular given detuning, the achieved microwave frequency increased linearly with the injected power due to frequency pushing effects. This illustrates once more the highly tunability nature of the proposed microwave signal generator. Another important parameter to determine the quality of the proposed system is the RF power of the generated signals. Figure 4(b) plots, also in a 3D map, the evolution of the RF power of the generated microwave signals as a function of P_{inj} and Δf. Figure 4(b) shows that the RF power varies considerably depending on the initial detuning and injected power configured. Values ranging from approx. −25 to −70 dBm, as directly measured from the ESA used in the experimental setup, were obtained for the generated microwave signals. Highest RF powers were achieved for the 4 - 20 GHz frequency detuning range. Medium RF powers were measured for initial detunings from 20 to 28 GHz and lower RF powers were measured for detuning below 4 GHz and over 28 GHz. Combining the results in Figs. 4(a) and 4(b), it can be concluded that relatively high RF power (exceeding −40 dBm) microwave signals with oscillation frequencies ranging from 5 to 23 GHz can be generated when Δf is set in the range of 4 – 20 GHz. Mid-amplitude RF signals with RF power over −50 dBm and oscillation frequencies from 23 – 30 GHz could be generated when the detuning between ML and SL is set within 18 – 26 GHz.

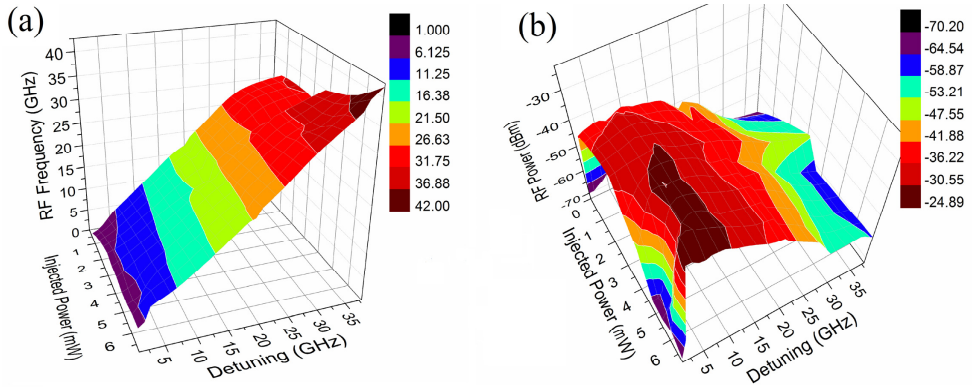

Fig. 4. Frequency (a) and RF power (b) of the generated microwave signals vs. Δf and P_{inj}.

4. Conclusions

In this work tunable microwave signal generation has been demonstrated with an optically-injected 1310nm-QD DFB laser. High quality microwave signals from below 1 to over 40 GHz can be constructed with the system proposed by simply controlling the injection strength and the initial frequency detuning between ML and SL. Furthermore, the use of the QD DFB laser of this work offers the advantage, compared to QW devices, that its stability map is characterized by a vast undisrupted region of period 1 dynamics in the positive frequency range, which enables continuous tuning. This entire region can be used for microwave signal generation without the interference of other regions of unwanted dynamics. These exciting results added to the simple experimental configuration used and the theoretically superior

#185425 - $15.00 USD Received 15 Feb 2013; revised 3 Apr 2013; accepted 15 Apr 2013; published 25 Apr 2013

properties of nanostructure laser offers the potential for novel, inexpensive, simple and highly tunable microwave signal generators for use in many future technological applications.

Acknowledgments

This work has been funded in part by the European Commission under the Programme FP7 Marie Curie International Outgoing Fellowships (IOF) Grant PIOF-GA-2010-273822 and the Air Force Office of Scientific Research Grant FA9550-10-1-0276 and AFRL Contract FA8750-06-1-0085.

#185425 - $15.00 USD Received 15 Feb 2013; revised 3 Apr 2013; accepted 15 Apr 2013; published 25 Apr 2013